Available online at www.sciencedirect.com
SCIENCE DIRECT®
Physica E 16 (2003) 253–258
PHYSICA E
www.elsevier.com/locate/physe

# Magnetic field effects on intersubband transitions in a quantum nanostructure

Tapash Chakraborty[a,*,1], V.M. Apalkov[b]

[a] *Max-Planck-Institut für Physik komplexer Systeme, Nöthnitzer Strasse 38, 01187 Dresden, Germany*
[b] *Physics Department, University of Utah, Salt Lake City, UT 84112-0830, USA*

Received 19 August 2002; accepted 11 October 2002

**Abstract**

We report on our theoretical studies of the magnetic field effects on intersubband transitions in quantum dots (QDs) embedded in a quantum cascade structure subjected to a strong magnetic field applied perpendicular to the QD plane. The peaks of the emission spectra calculated for QDs containing a few interacting electrons indicate that there is a correlation between the non-monotonic behavior of the maximum value of the emission spectrum as a function of the applied magnetic field and the field dependence of the low-lying energy spectra of the dots.


*Keywords:* Intersubband transitions; Quantum dots; Quantum cascade laser

Rapid developments in modern epitaxial growth techniques have enabled researchers to create structures on the nanometer scale where many fascinating new physical phenomena have been discovered [1]. In this context, quantum dots (QDs) represent the ultimate reduction in the dimensionality of a nanoscopic device. Here electrons are confined in all directions, and they occupy spectrally sharp energy levels like those found in atoms [2,3]. An external magnetic field perpendicular to the QD plane is a very powerful means to identify the quantum number of states in a dot. The basic energetics of an electron in a parabolic confinement—suitable for a QD model—subjected to an external magnetic field is known since the early days of quantum mechanics. The single-electron energies in this case are written as [4,5] $\mathscr{E}_{nl} = (2n + 1 + |l|)\hbar\Omega - \frac{1}{2}l\hbar\omega_c$, where $\Omega = (\frac{1}{4}\omega_c^2 + \omega_0^2)^{1/2}$, $\omega_c = eB/m^*c$ is the cyclotron frequency in a magnetic field $B$, and $\hbar\omega_0$ is the confinement energy. The single-electron wave function (without the normalization constant) is written as $\varphi_{nl} = r^{|l|}\exp(-il\theta)L_n^{|l|}(r^2/2a^2)$ where the effective magnetic length $a$ is given by $a^2 = \hbar/(2m^*\Omega)$, and $L_n^{|l|}$ is a Laguerre polynomial. The quantum number $-l$ is the angular momentum and the quantum number $n$ is related to the Landau quantum number $N = n + (|l| - l)/2$ (usually referred to as Fock–Darwin level index [2,3]). In the absence of any confinement $N$ becomes the familiar Landau level index, and $\mathscr{E} = (N + \frac{1}{2})\hbar\omega_c$. In the presence of a confinement, $\mathscr{E}_{nl}$ is a function of both $n$ and $l$ [6]. Several experimental groups have reported observation of these features in QDs [7]. Introduction of interelectron interaction

* Corresponding author.
*E-mail address:* tapash@mpipks-dresden.mpg.de (T. Chakraborty).
[1] Also at: Institute of Mathematical Sciences, Chennai 600113, India.

1386-9477/03/$ - see front matter © 2002 Elsevier Science B.V. All rights reserved.
PII: S1386-9477(02)00674-4

in the theoretical treatment of a many-electron dot results in magic quantum numbers [6] that occur due to competition between the confinement and interaction energies. Theoretical studies of the influence of the confinement and interaction in the presence of a magnetic field on *intersubband transitions* might be important for exploration of the energetics of QDs as in the case of quantum wells (for a review, see e.g., Ref. [8]; experimental work in a similar spirit but based on tunable intersublevel transitions in self-assemble QDs was reported in Ref. [9]). Moreover, in quantum wells, intersubband transitions are useful routes toward developing designer optical properties and quantum well engineering [10], and it may as well be the case with the dots. There is, however, an important difference between the wells and the dots in a similar situation. For a quantum well in a perpendicular magnetic field, the subbands quantize into a ladder of Landau levels and only cyclotron transitions are possible (unless, of course, one applies a parallel field or a magnetic field that is tilted from the direction normal to the electron plane [8,11]). On the other hand, in QDs confinement and magnetic field lead to Fock–Darwin energy levels at low fields [2,3], and cyclotron transitions appear only at very high fields where the Fock–Darwin levels merge to form the Landau levels [2–5].

In this paper, we investigate the magnetic field effects on intersubband transitions in a QD. In order that these results might find use in a realistic nanostructure, we have explored a quantum cascade type of structure where in place of the quantum wells, the active regions contain QD-like confinement. We should, however, point out that the effects we have uncovered here are quite general since they are largely dictated by the energy spectra of the dots, as demonstrated below. Quantum cascade laser (QCL) is a nanostructured light source in the mid-infrared range ($\simeq$3.5–20 μm) ([12], for a review, see e.g., Ref. [13]) which has proven to have vast application potentials [14] ranging from gas sensing [15,16] to free-space optical data transmission [17]. In these systems, optical transition occurs between quantized conduction band states (intersubband transition) of a multiple quantum well structure. A quantum-dot cascade laser (QDCL) is predicted to exhibit a large blueshift in the luminescence spectra [18] and is expected to be useful in tuning the laser by injection of individual electrons in the dot.

The single-electron Hamiltonian for our system has the form

$$\mathscr{H}' = \frac{1}{2m^*}(p_x - eBy/2c)^2 + \frac{1}{2m^*}(p_y + eBx/2c)^2 + \frac{p_z^2}{2m^*} + V_{\text{plane}}(x,y) + V_{\text{conf}}(z), \tag{1}$$

where $B$ is the applied magnetic field in the $z$-direction and the confinement potential in that direction is [11,18]

$$V_{\text{conf}}(z) = -eFz + \begin{cases} 0 & \text{for wells,} \\ U_0 & \text{for barriers,} \end{cases}$$

with $F$ being the electric field in the $z$-direction.

We model the QDs in the active layers of the QCL by assuming parabolic confinement potential in the $xy$-plane: $V_{\text{plane}}(x,y) = \frac{1}{2}m^*(\omega_x^2 x^2 + \omega_y^2 y^2)$, where $\omega_x$ and $\omega_y$ are the confinement energies in the $x$- and $y$-direction, respectively, corresponding to the oscillator lengths of $l_x = (\hbar/m^*\omega_x)^{1/2}$ and $l_y = (\hbar/m^*\omega_y)^{1/2}$. The single-electron Hamiltonian can then be rewritten as

$$\mathscr{H}' = \mathscr{H}_z + \mathscr{H}_x + \mathscr{H}_y + \mathscr{H}_{xy}, \tag{2}$$

where

$$\mathscr{H}_x = \frac{p_x^2}{2m^*} + \frac{m^*}{2}\left(\omega_x^2 + \frac{1}{4}\omega_c^2\right)x^2,$$

$$\mathscr{H}_y = \frac{p_y^2}{2m^*} + \frac{m^*}{2}\left(\omega_y^2 + \frac{1}{4}\omega_c^2\right)y^2,$$

$$\mathscr{H}_z = \frac{p_z^2}{2m^*} + V_{\text{conf}}(z),$$

and

$$\mathscr{H}_{xy} = \frac{\omega_c}{2}(xp_y - yp_x).$$

As a first step we calculate eigenfunctions and eigenvalues of the single-electron Hamiltonian $\mathscr{H}_x + \mathscr{H}_y + \mathscr{H}_z$. The eigenfunctions are the product of eigenfunctions of corresponding one-dimensional Hamiltonians:

$$\Psi_{nmk} = \varphi_{x,n}(x)\varphi_{y,m}(y)\chi_k(z),$$

where $\varphi_{x,n}(x)$ and $\varphi_{x,n}(x)$ are eigenfunctions of harmonic oscillators with frequencies $(\omega_x^2 + \omega_c^2/4)^{1/2}$ and $(\omega_x^2 + \omega_c^2/4)^{1/2}$, respectively. The subband functions $\chi_k(z)$, are calculated numerically. Then for each

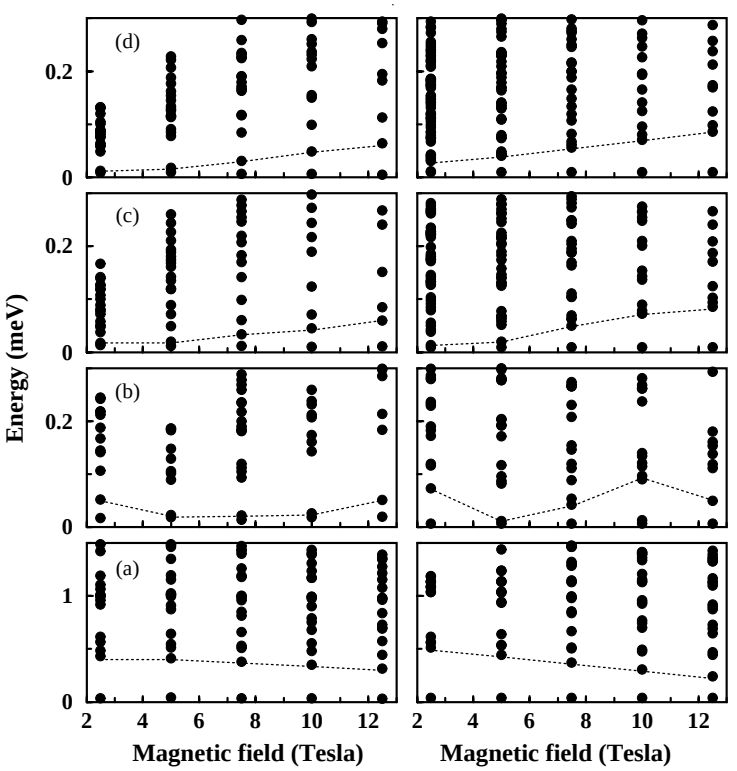


Fig. 1. The energy spectra of a two-electron circular ($l_x = l_y$) QD. The QD sizes (in nm) considered here are: (a) (5,5), (b) (10,10), (c) (15,15) and (d) (20,20). The left column corresponds to the interacting system while the right one is for the non-interacting systems.

subband $k$, we diagonalize the Hamiltonian $\mathscr{H}_{xy}$ in a subspace $\varphi_{x,n}(x)\varphi_{y,m}(y)$, where $n$ and $m$ are less than 20. As a result, we find the eigenfunctions, $\Psi_{j,k}(x,y,z)$, and eigenstates, $E_{j,k}$, of single-electron Hamiltonian (1). In our calculations that follow, we consider only two subbands in the $z$-direction ($k = 1, 2$) and for a given $k$ all possible states in the $xy$-plane with the condition, $E_{jk} < U_0$.

From the single-electron basis functions, we construct the $N$-electron (spinless) basis

$$\Phi_{n_i m_i k_i}(\mathbf{r}_1, \ldots, \mathbf{r}_N) = \mathscr{A}\Psi_{n_1 m_1 k_1}(\mathbf{r}_1)\cdots\Psi_{n_N m_N k_N}(\mathbf{r}_N), \quad (3)$$

where $\mathscr{A}$ is the antisymmetrization operator. The total many-electron Hamiltonian is written as

$$\mathscr{H} = \sum_{i=1}^{N} \mathscr{H}'_i + \sum_{i<j}^{N} V(|\mathbf{r}_i - \mathbf{r}_j|),$$

where $\mathscr{H}'$ is given by Eq. (2). For interelectron interactions we consider the Coulomb interaction $V(|\mathbf{r}_i - \mathbf{r}_j|) = e^2/\varepsilon|\mathbf{r}_i - \mathbf{r}_j|$, where $\varepsilon$ is the background dielectric constant. The Hamiltonian matrix is then calculated in basis (3). The eigenvalues and eigenfunctions were calculated by exact (numerical) diagonalization of the Hamiltonian matrix.

In the initial state (before optical emission) all electrons are in the second subband, $k = 2$. In the final state (after optical emission) one electron is in the first subband, $k = 1$, and all other electrons are in the second subband, $k = 2$. The intensity of optical transitions is found from the expression

$$\mathscr{I}_{if}(\omega) = \frac{1}{Z}\sum_{if}\delta(\omega - E_i + E_f) \times \left|\int \chi_1(z) z \chi_2(z)\,\mathrm{d}z \int \Phi_i^*(x_1 y_1, \ldots, x_N y_N)\right.$$

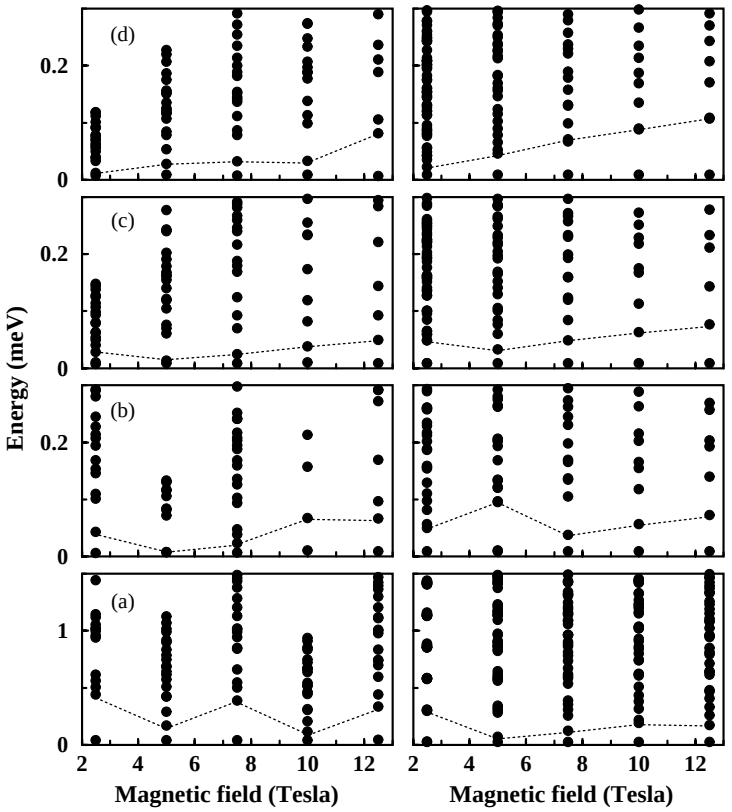


Fig. 2. The energy spectra of a two-electron non-circular ($l_x \neq l_y$) QD. The dot sizes (in nanometers) are: (a) (5,10), (b) (10,15), (c) (15,20) and (d) (20,25). The left column corresponds to the interacting system while the right one is for the non-interacting systems.

$$\times \Phi_f(x_1 y_1, \ldots, x_N y_N)$$

$$\times \, \mathrm{d}x_1 \, \mathrm{d}y_1 \cdots \mathrm{d}x_N \, \mathrm{d}y_N \Big|^2$$

$$\times \exp(-\beta E_i),$$

where $Z = \sum_i \mathrm{e}^{-\beta E_i}$ is the partition function and $\beta = 1/kT$. In all our computation, we take $T = 20$ K. We present below our theoretical results for a dot containing two electrons.

In Fig. 1 the energy spectra of circular ($l_x = l_y$) QDs containing two electrons are shown for different values of the oscillator strength and different values of the magnetic field. The results in the left column correspond to a system of interacting electrons, while those in the right column are for the non-interaction systems. Similar energy spectra are shown in Fig. 2 for elliptical QDs ($l_x \neq l_y$). Clearly, the effect of interaction on the energy spectra becomes more pronounced for larger QDs, which is due to the fact that for a larger QD the interlevel separation for a single-electron system becomes smaller, i.e. the interaction becomes more important. Another observation is that at a given value of the magnetic field the interaction between electrons tends to decrease the excitation gap (separation between the low-lying energy levels). This effect manifests itself in the emission spectra. In Fig. 3, positions of the maximum of the luminescence spectra as a function of the applied magnetic field are shown for circular and elliptical QDs. For QDs of a small size ($l_x = l_y = 5$ nm and $l_x = 5$ nm, $l_y = 10$ nm) the effect of the magnetic field on the emission peaks is negligible. This is in good agreement with the energy spectra of a circular dot (Fig. 3(a)), where a large gap is present at all values of the magnetic field.

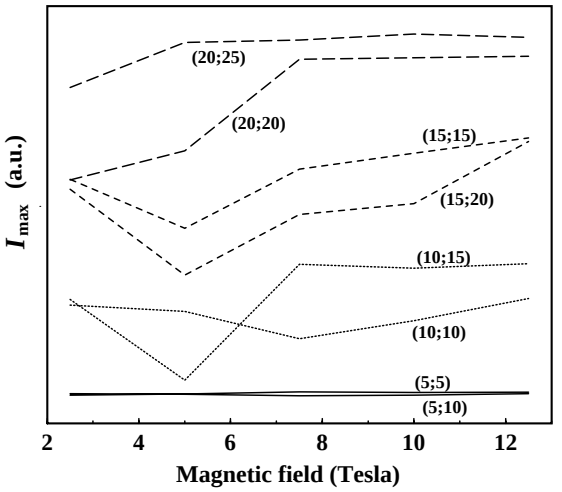


Fig. 3. The emission peak as a function of magnetic field for circular and non-circular QDs. The numbers next to the lines in the figure correspond to the size of the dot $(l_x, l_y)$.

With increasing size of the QD a well pronounced downward cusp is developed for a magnetic field close to 5 T. This cusp is observed for a size of the QD close to 15 nm. In fact, there is an interesting correlation between the appearance of the cusp and the energy spectra of the QD system. Such a non-monotonic dependence of the maximum value of the emission line on the magnetic field is observed whenever there is a non-monotonic dependence of the energy gap on the magnetic field. The cusps correspond to the smallest value of the gap. Indeed, there is a minimum of the energy gap at $B = 5$ T for $l_x = 10$ nm, $l_y = 15$ nm system (in Fig. 2(b), and also in Fig. 1(b), the energy gap is so small that two points, ground and excited states in the figure almost coincide). This minimum corresponds to the minimum in Fig. 3. At the same time the energy gap for the circular dot ($l_x = 10$ nm, $l_y = 10$ nm) has a weak dependence on the magnetic field which results in an almost monotonic field dependence in Fig. 3. With a further increase in size of the dots the energy gap dependence on magnetic field becomes more monotonic and the cusps disappear.

The specific feature of the system under consideration is that the main transitions are the transitions between the ground state of the initial system and the exited states of the final system. This can be understood from an analysis of the non-interacting system. For the non-interacting two-electron system, electrons in the initial ground state occupy two lowest Fock–Darwin states (Fig. 4) of the second subband. The transitions are allowed only to the excited state of the final system, where the electron in the second subband is in the ground Fock–Darwin state and the electron in the first subband is in the first excited Fock–Darwin state. The transition to the ground state, in which both electrons are in the ground Fock–Darwin state of the corresponding subbands, is forbidden. This transition is allowed only due to the non-parabolicity of the energy spectrum, and therefore its probability is very low. It is easy to see that the height of the emission peak for the non-interacting system does not depend on the magnetic field.

The interelectron interaction mixes the energy states both in the initial and in the final non-interacting systems. As a result the emission peak becomes broad and has a lower height compared to that for the non-interacting system. If the electron–electron interaction in the initial and in the final systems would be the same then antisymmetric many-electron states would be identical in the initial and the final systems, and as a result, the height of the emission peak would not depend on the magnetic field. In the present case, interactions between the electrons in the initial system (electrons are in the same subband) and in the final system (electrons are in the different subbands) are different. If this difference has a weak effect on the many-electron states then the height of the emission peak has a weak dependence on the magnetic field. Conversely, the height of the emission peak has a strong magnetic field dependence if the states of the many-electron system are very sensitive to the interelectron interaction. Such sensitivity is partially determined by the energy gaps in the non-interaction system. This is the origin of the correlation between the emission peaks and energy spectra.

To summarize, we have explored the magnetic field effects on intersubband transitions in QDs embedded in a quantum cascade laser structure. The calculated emission spectra for QDs containing a few interacting electrons indicate that the behavior of the emission peaks as a function of the applied magnetic field directly reflects the field dependence of the low-lying energy gap of the QD structure.

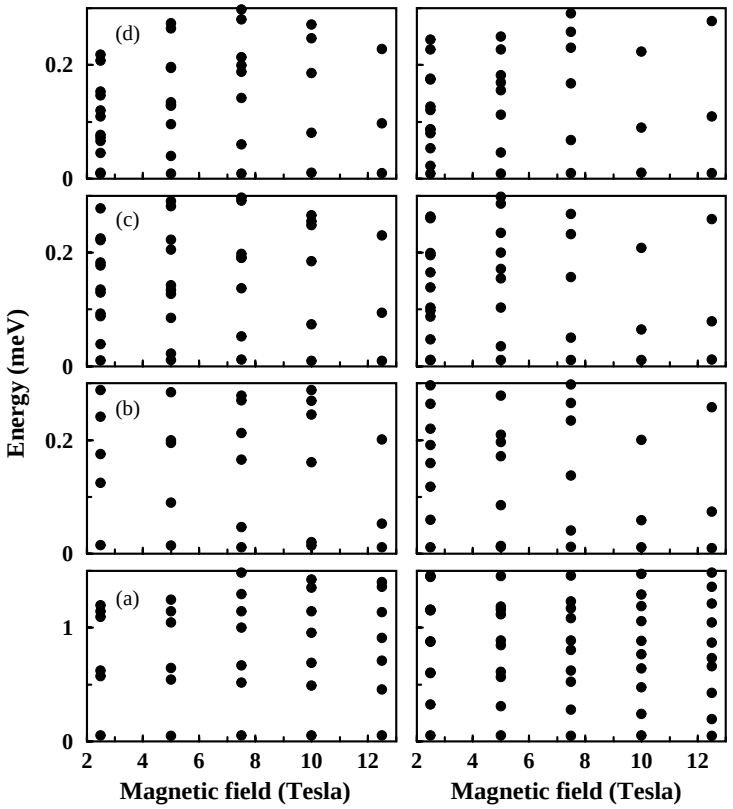


Fig. 4. The Fock–Darwin energy spectra of a two-electron QD in the active layers of a QCL. The QD sizes (in nm) considered here are: (a) (5,5), (b) (10,10), (c) (15,15) and (d) (20,20). The left column corresponds to the circular dot while the right one is for the non-circular dot.

## References

[1] T. Chakraborty, F. Peeters, U. Sivan (Eds.), Nano-Physics & Bio-Electronics: A New Odyssey, Elsevier, Amsterdam, 2002.
[2] T. Chakraborty, Comments Condens. Matter Phys. 16 (1992) 35.
[3] T. Chakraborty, Quantum Dots, Elsevier, Amsterdam, 1999.
[4] V. Fock, Z. Physik 47 (1928) 446.
[5] C.G. Darwin, Proc. Cambridge Philos. Soc. 27 (1930) 86.
[6] P.A. Maksym, T. Chakraborty, Phys. Rev. Lett. 65 (1990) 108.
[7] D.G. Austing, et al., in: T. Chakraborty, F. Peeters, U. Sivan (Eds.), Non-Physics & Bio-Electronics: A New Odyssey, Elsevier, Amsterdam, 2002;
D. Mowbray, J. Finley, in: T. Chakraborty, F. Peeters, U. Sivan (Eds.), Non-Physics & Bio-Electronics: A New Odyssey, Elsevier, Amsterdam, 2002 (see also Refs. [2,3] for earlier references).
[8] M. Helm, Semicond. Semimet. 62 (2000) 1.
[9] R. Leon, et al., Phys. Rev. B 58 (1998) R4262.
[10] K.L. Wang, R.P.G. Karunasiri, in: M.O. Manasreh (Ed.), Semiconductor Quantum Wells and Superlattices for Long-Wavelength Infrared Detectors, Artech House, Norwood, MA, 1993;
B.F. Levine, J. Appl. Phys. 74 (1993) R1;
A.G.U. Perera, J.W. Choe, M.H. Francombe, Thin Films 23 (1997) 217.
[11] V. Apalkov, T. Chakraborty, Appl. Phys. Lett. 78 (2001) 1973.
[12] J. Faist, et al., Science 264 (1994) 553.
[13] C. Gmachl, et al., Rep. Prog. Phys. 64 (2001) 1533.
[14] F. Capasso, et al., Phys. World 12 (1999) 27;
F. Capasso, et al., Phys. Today 55 (2002) 34.
[15] F. Capasso, et al., Opt. Photonics News 10 (1999) 31;
C. Gmachl, et al., IEEE Circuits Devices 16 (2000) 10.
[16] C.R. Webster, et al., Appl. Opt. 40 (2001) 321.
[17] R. Martini, et al., Electron. Lett. 37 (2001) 191;
S. Blaser, et al., Electron. Lett. 37 (2001) 778.
[18] V. Apalkov, T. Chakraborty, Appl. Phys. Lett. 78 (2001) 1820;
V. Apalkov, T. Chakraborty, Physica E 14 (2002) 294.